

The NLTE Barium Abundance in Dwarf Stars in the Metallicity Range of $-1 < [\text{Fe}/\text{H}] < +0.3$

S. Korotin^{1*}, T. Mishenina¹, T. Gorbaneva¹, and C. Soubiran²

¹*Astronomical Observatory of Odessa National University, and Isaac Newton Institute of Chile Odessa branch, Odessa, Ukraine*

²*Université Bordeaux 1, CNRS - Laboratoire d'Astrophysique de Bordeaux, UMR 5804, 33370 Floirac, France.*

Accepted. Received ; in original form

ABSTRACT

We present the results of determination of the barium abundance considering the non-LTE (NLTE) effects in 172 dwarf stars in the metallicity range of $-1 < [\text{Fe}/\text{H}] < +0.3$, assigned to different Galactic substructures by kinematic criteria. We used a model of the Ba atom with 31 levels of Ba I and 101 levels of Ba II. The atmosphere models for the investigated stars were computed using the ATLAS9 code modified by new opacity distribution functions by Castelli & Kurucz (2004). The NLTE profiles of the unblended Ba II (4554 Å, 5853 Å, 6496 Å) were computed and then compared to those observed. The line 6141 Å was also used, but with an allowance for its correlation with the iron line. The average barium abundances in the thin and thick discs are 0.01 ± 0.08 and -0.03 ± 0.07 , respectively. The comparison to the calculations of the Galactic chemical evolution by Serminato et al. (2009) was conducted. The trend obtained for the Ba abundance versus $[\text{Fe}/\text{H}]$ suggests a complex barium production process in the thin and thick discs.

Key words: stars: abundances – stars: late-type – Galaxy: disc – Galaxy: evolution.

1 INTRODUCTION

Barium is one of the elements formed by the neutron capture processes; it is an important component in nucleosynthesis by the neutron capture reactions, as well as in reconstruction of its evolution in the Galaxy and the Galactic chemical evolution as a whole. The neutron capture reactions can proceed in two ways, depending on the neutron flux density: as a *slow* process (s-process) or as a *rapid* process (r-process). Based on the classical model describing the solar abundance distribution of s-process elements with three exponential distributions of neutron exposures (Kappeler et al. 1989), the s-process is divided into three components: the *main* s-component is produced in the asymptotic giant branch (AGB) stars (isotopes with A from 90 to 208); the *weak* s-component is provided mainly by massive stars that explode later on as Supernovae (isotopes with A up to 90). The third strong s-component was introduced to reproduce 50% of ²⁰⁸Pb (Kappeler et al. 1982). The origin of the rapid r-process is still discussed now. The principal sources of the r-process nuclei production might be massive stars (Woosley et al. 1994) or yields from coalescence of two neutron stars (sometimes, black hole and neutron star Freiburghaus et al. 1999; Surman et al. 2008). Such s-

process elements as Sr, Y, Zr are labeled as *light* s-elements (ls); barium heads the group of *heavy* s-elements (hs) (Ba, La, Ce, Nd, Sm) (that corresponds to the first and the second peaks of the s-process elemental abundance curve). According to the modern view on the role of the third dredge-up and multiplicity of neutron-capture contributions, the AGB stars bring the most to the s-elements enrichment at near-solar metallicities (for example, Cristallo et al. 2009). The estimates of s-process relative contribution to the solar Ba abundance, conducted in series of works, are rather similar - from 81% to 85% (Kappeler et al. 1989, Serminato et al. 2009). However, the barium abundance variations relative to metallicity draw particular attention. As a rule, with diminishing metallicity, a decrease in the ratio of Ba abundance relative to iron $[\text{Ba}/\text{Fe}]$ is observed with an marked dispersion of $[\text{Ba}/\text{Fe}]$ at $[\text{Fe}/\text{H}]$ within -3 - -4 dex (François et al. 2007, Frebel 2010). At the indicated metallicities, it is an r-process, and therefore massive stars, that contribute to the barium enrichment the most (Argast et al. 2004, Cestito et al. 2006). The increasing number of less massive AGB stars with the growing metallicity in the Galaxy changes proportions of r- and s-processes contribution to the barium enrichment. As a result, at the near-solar metallicity, the $[\text{Ba}/\text{Fe}]$ overabundance relative to the solar ratio is noticed. The barium abundance in the stars with metallicity from -1 to $+0.3$ has been investigated in a number of studies

* E-mail: serkor@skyline.od.ua

(Mashonkina & Gehren 2000, Mashonkina & Gehren 2001, Bensby et al. 2005, Reddy et al. 2006). On considering the dependence of the barium abundance on metallicity, the presence of the [Ba/Fe] peak at [Fe/H] of about -0.2 dex calls attention; that peak has been discovered earlier in the classical research by Edvardsson et al. (1993). In the recent studies by Bensby et al. (2005), and Reddy et al. (2006), that investigated a great number of stars of the thick and thin discs, the lower barium abundance in the thick disc stars relative to that in the thin disc members was obtained; but as per research data by Bensby et al. (2005), the above mentioned peak was noticed only in the thin disc stars. As stated by the modern conception, the interstellar medium, where dwarf stars with metallicity from -1 to $+0.3$ dex (those are thick and thin discs stars) were born, has been contaminated with the products of evolution of several generations of stars; thus, to adequately reconstruct the enrichment history, it is necessary to use a Galactic evolution model that allows for processes changing the abundance of chemical elements in the course of the evolution. It is known that the abundance of barium can deviate from the local thermodynamic equilibrium value (Mashonkina et al. 1999, Andrievsky et al. 2009), especially in metal-poor stars. In the present study, we used the NLTE approach to determine more accurately the barium abundance in 172 dwarf stars that earlier had been kinematically assigned to the thick and thin discs (Mishenina et al. 2004), and also to specify and analyze its behaviour in the stars of the thin and thick Galactic discs in order to compare with the Galactic evolution models.

2 OBSERVATIONS AND SELECTION

The spectra of 172 stars (F-G-K V) were obtained in the region of $\lambda\lambda 4400 - 6800 \text{ \AA}$ with the signal-to-noise ratios S/N about 100-300 using the 1.93 m telescope at Observatoire de Haute-Provence (OHP, France) equipped with the échelle-spectrograph ELODIE (Baranne et al. 1996). The resolving power R was 42000. The initial spectra processing was made online through the telescope (Katz et al. 1998). The studied spectra subsequent processing (including the continuous spectrum level set up, the development of a dispersion curve, the measurement of equivalent widths EW, etc.) was performed using the DECH20 software package (Galazutdinov 1992).

To select the stars that belong to the thin and thick discs, we used a kinematic approach to assign the target stars by the probability of their membership in either the thin or thick discs on the base of their spatial velocities, kinematic parameters of the discs, and the percentage of stars in each disc. More details can be found in Mishenina et al. (2004), Soubiran & Girard (2005).

3 DETERMINATION OF PARAMETERS

The atmospheric parameters of the target stars were determined in the previous studies (Mishenina & Kovtyukh 2001, Mishenina et al. 2004).

The effective temperatures T_{eff} were estimated by the calibration of the ratio of the central depths of the lines

with different potentials of the lower bf level in the region of metallicity $[\text{Fe}/\text{H}] > -0.5$ dex developed by Kovtyukh et al. (2003) with a typical accuracy better than 10 K. The effective temperatures for the more metal-poor stars ($[\text{Fe}/\text{H}] < -0.5$) were determined by the fitting of the H_{α} line wings (Mishenina & Kovtyukh 2001). To testify the temperatures scales of Kovtyukh et al. (2003) and Mishenina & Kovtyukh (2001) we have compared in Mishenina et al. (2004) of the temperatures determined by us with the results of by Alonso et al. (1996), Blackwell & Lynas-Gray (1998), and di Benedetto (1998). Our temperature scale is slightly hotter than their by $\sim 20 - 30$ K, as mentioned in Kovtyukh et al. (2003), but the dispersion is satisfactory (~ 80 K).

The surface gravities $\log(g)$ were determined by two methods for the stars with T_{eff} higher than 5000 K (namely, by the iron ionisation balance and the parallax). For the cooler stars the parallax method was only used. Allende Prieto et al. (1999) have analysed this two methods and concluded that astrometric and spectroscopic (iron ionization balance) gravities were in good agreement in the metallicity range $-1.0 < [\text{Fe}/\text{H}] < +0.3$. We compared (Mishenina et al. 2004) our adopted surface gravities to those determined astrometrically by Allende Prieto et al. (1999) and obtain a mean difference and standard deviation of -0.01 and 0.15 respectively for 39 stars in common. This is consistent with an accuracy of 0.1 dex on our estimated spectroscopic gravities.

The microturbulent velocity V_t was derived considering that the iron abundance $\log A(\text{Fe})$ obtained from the given Fe I line, is not correlated with the equivalent width EW of that line.

The adopted value of the metallicity [Fe/H] is the iron abundance obtained from Fe I lines. As it is known, the neutral iron lines deviate from the local thermodynamic equilibrium (LTE) and that consequently affects the iron abundances obtained from those lines. However, in the temperature and metallicity ranges of the target stars, the NLTE corrections do not exceed 0.1 dex (Mashonkina et al. 2010).

The comparison of the determined atmospheric parameters to the data obtained by other authors is presented in previous studies (Mishenina et al. 2004). The external accuracy of the effective temperature is $\Delta T_{\text{eff}} = \pm 100$ K and of the surface gravity is $\Delta \log(g) = \pm 0.2$ dex.

4 DETERMINATION OF THE BARIUM ABUNDANCE, THE MODEL OF ATOM

The barium abundance in dwarf stars is determined from Ba II 4554 Å, 5853 Å, 6141 Å, and 6496 Å lines under the non-LTE approximation.

The used model of the Ba atom is described in detail by Andrievsky et al. (2009). The model contains 31 levels of Ba I, 101 levels of Ba II with $n < 50$, and the ground level of Ba III. In the detailed study, we included 91 bound-bound transitions between the first 28 levels of Ba II with $n < 12$ and $l < 5$. To check the completeness of our atomic model we performed the test calculations. The test calculations that take into account only transitions between the first 20 levels of Ba II have shown that decrease of the number of considered levels practically does not affect the lines of interest.

Some uncertainty of the NLTE analysis of the bar-

ium spectrum is caused by the lack of information on the photoionization cross sections for different levels. We used the results of the scaled Thomas-Fermi method application (Hofsaess 1979).

The effective collision strengths for electron excitation for the transitions between the first levels ($6s^2S$, $5d^2D$ and $6p^2P^0$) were used following to Schoening & Butler (1998). The experimental cross-sections for the transitions $6s^2S - 7s^2S$ and $6s^2S - 6d^2D$ were taken from Crandall et al. (1974). The collisional rates for the transitions between sublevels $5d^2D$, $6p^2P^0$ and $7s^2S$, $6d^2D$, as well as between $7s^2S$ and $6d^2D$ were estimated by the corresponding formula from Sobelman et al. (1981). For the rest of the allowed transitions, we applied the van Regemorter (1962) formula, while the Allen's formula (Allen 1973) was used for the forbidden transitions. The collisional ionization rate from the ground level of Ba II was computed with the appropriate formula from Sobelman et al. (1981).

The collisions with hydrogen atoms were considered using the Steenbock & Holweger (1992) formula with a correction factor of 0.1 that was derived empirically by analyzing the profiles of the Ba lines in the solar spectrum. The change of this coefficient in the range from one to zero does not affect the resonance line profile in the solar spectrum, while subordinate lines show variation of the equivalent width in the range 5.5%-7%.

The odd barium isotopes have hyperfine splitting of their levels and thus several HFS components for each line Rutten (1978). Therefore, the line 4554 Å and 6496 Å was fitted in the solar spectrum (see Fig. 1) by adopting the even-to-odd abundance ratio of 82:18 (Cameron 1982). The hyperfine splitting for the lines 5853 Å and 6141 Å is insignificant. The parameters of the analyzed lines are given in Table 1. We determined Γ_{vdw} by fitting the computed line profiles to those observed in the solar spectrum. These estimates agree very well with results of theoretical calculations Barklem et al. (2000) for resonance line (the difference is only 0.05 dex) and for the lines 6494 and 5141 (the difference is about 0.10 dex). Nevertheless the 5853 line wings were fitted to observed profile only with $\Gamma_{vdw} = -7.19$, that is 0.39 dex larger than the value adopted in Barklem et al. (2000). At the same time we took into account that this line is blended with weak Fe I line.

The estimates of the radiative broadening for the lines 4554, 5853 and 6496 Å are taken from Mashonkina & Bikmaev (1996); for the line 6141 Å - from the Vienna Atomic Line Database (VALD). Calculated barium line profiles in de Solar spectrum (Kurucz et al. 1984) agree well with observed profiles if we use barium abundance 2.17 (in good agreement with the estimation of the solar abundance of barium of Asplund et al. (2005)).

The NLTE profiles of the barium lines were computed using a modified version of the MULTI code (Carlsson 1986). The modifications applied are described in Korotin et al. (1999).

The Ba II lines are to some extent blended with other metallic lines (especially the line 6141 Å), to compare the NLTE barium line profiles to those in the observed spectrum, it is necessary to use a combination of the NLTE and LTE synthetic spectra. It was made with the updated SynthV code (Tsymbal 1996) that was designed for synthetic spectrum calculations under the LTE. This code, as well as

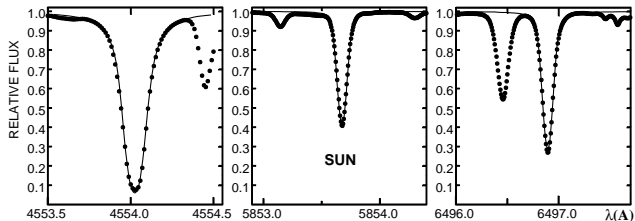


Figure 1. Profile fitting in the solar spectrum.

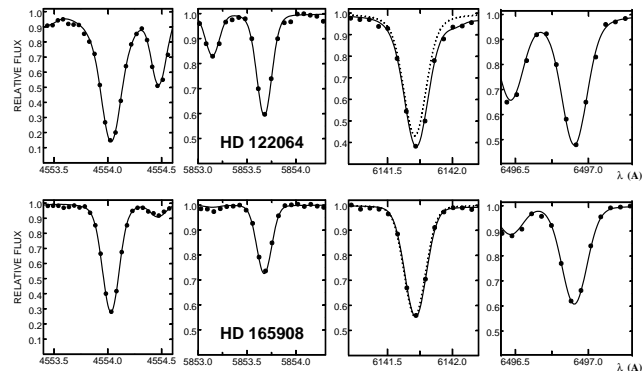


Figure 2. Profile fitting in the stellar spectrum. The line 6141 Å is blended with the iron line (the dot line - is the barium line profile).

MULTI code (our version), is based on the opacities from ATLAS9. The test calculations of the LTE profiles generated by SynthV and MULTI showed an excellent agreement.

Using the indicated program, we computed synthetic spectra for the selected regions, comprising the target Ba II lines, on having taken into account all lines of each region listed in the VALD. Specifically for the barium lines, the corresponding b -factors (factors of deviation from the LTE level populations), computed by the MULTI, were included into the SynthV and subsequently applied in calculation of the barium line source function.

For the computations we used the stellar atmosphere models computed using the ATLAS9 program with new ODF tables (Castelli & Kurucz 2004) without overshooting for each star separately.

The accuracy of determination of the barium abundance in the investigated stars, obtained by fitting the synthetic spectra to those observed, is about 0.03 dex. Some examples of the profile fitting are presented on Fig. 2.

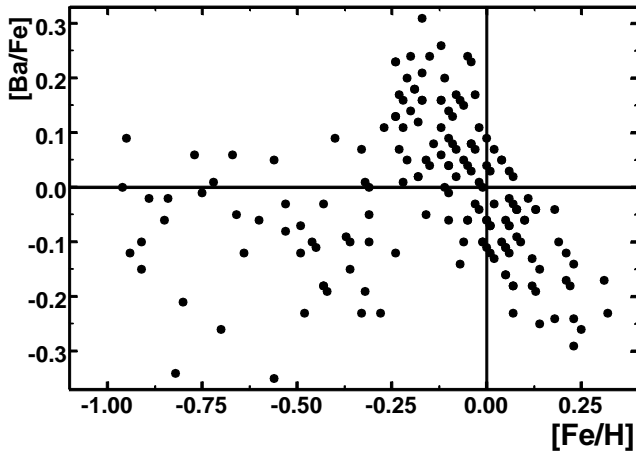
The total error of determination of the barium abundance is assumed to be 0.10-0.15 dex with an allowance of errors in estimations of effective temperature ($\Delta T_{\text{eff}} = \pm 100$ K), surface gravity ($\Delta \log(g) = \pm 0.2$), microturbulent velocity ($\Delta V_t = \pm 0.2$ km/s) and the determined value of metallicity ($\Delta [\text{Fe}/\text{H}] = \pm 0.10$).

Firstly, the barium abundance was determined from the only line 4554 Å under the LTE. The obtained results are given in Fig. 3. The shape of the obtained dependence between $[\text{Ba}/\text{Fe}]$ and $[\text{Fe}/\text{H}]$ appeared rather strange. A sharp peak and an intrinsic dispersion of the barium abundance ratio can be noticed.

The dispersion of the obtained barium abundance ratios

Table 1. Parameters of the barium lines.

$\lambda(\text{\AA})$	HFS	f	$\log \gamma_{\text{rad}}$	$\log \Gamma_{vw}$
	$\Delta\lambda, \text{m\AA}$	solar		
4554.03	0	0.597	8.20	-7.60
	18	0.081		
	-34	0.049		
5853.70	-	0.025	8.20	-7.19
6141.71	-	0.025	7.77	-7.47
6496.90	0	0.086	8.10	-7.47
	-4	0.012		
	9	0.007		

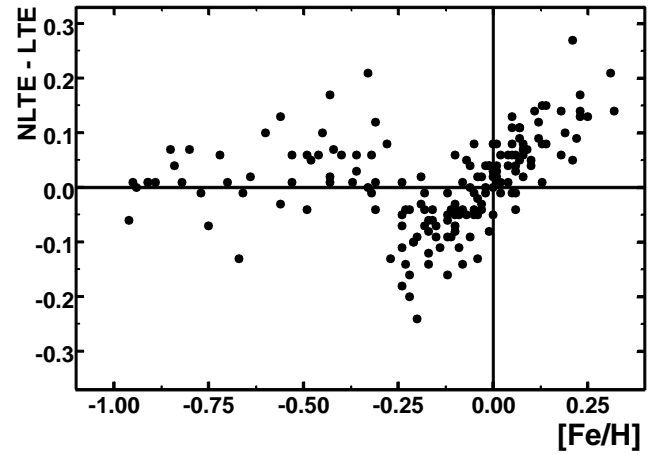
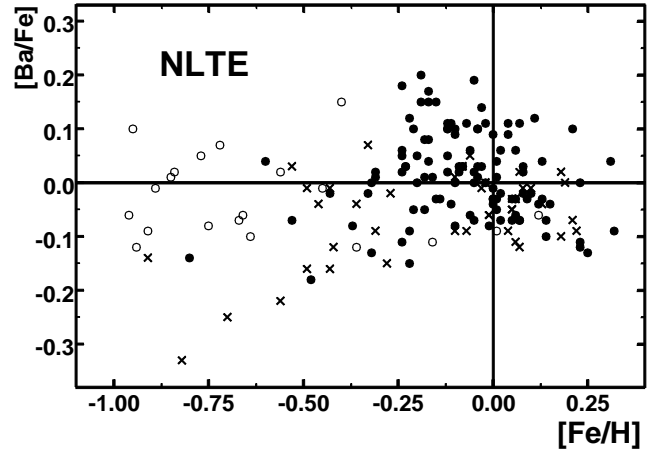
**Figure 3.** The LTE barium abundance (from the only 4554 Å line)

was appreciably decreased by considering deviations from the LTE and using the four Ba II lines; however, a small $[\text{Ba}/\text{Fe}]$ overabundance at $[\text{Fe}/\text{H}] = -0.2$ dex still remained. The results are given in Table. 3 and Fig. 4. The difference between the LTE and NLTE abundance determination is shown in the same figure. These differences equally conditioned by the two circumstances, firstly, by the use of four lines instead of one, and secondly, by the differences in the LTE and NLTE determinations. Let us note that the way of presentation of the barium abundance results in Fig. 3 (inclined parallel lines) is caused by the step discontinuity in synthetic spectrum fitting.

In Fig. 4, the thin disc stars are marked as filled circles, the thick disc stars - as open circles, the others - as crosses. Thus, it is evident that the LTE analysis of the only one 4554 Å line leads to the occurrence of systematic errors.

The results of the comparison of the obtained barium abundances and the atmospheric parameters to those of the other authors for common stars are given in Table 2, where ΔT_{eff} - the average effective temperature difference, $\Delta \log(g)$ - the average surface gravity difference, $\Delta [\text{Fe}/\text{H}]$ - the average metallicity difference, n - the number of common stars.

As is obvious from the mentioned comparison, the obtained values corroborate the external accuracy for T_{eff} and

**Figure 4.** The NLTE barium abundance and the NLTE corrections vs. metallicity. The thin disc stars are marked as filled circles, the thick disc stars - as open circles, the others - as crosses.**Table 2.** The results of the comparison of the obtained Ba NLTE abundance to the data from the LTE determination by Bensby et al. (2005) - B05, Reddy et al. (2006) - R06, and NLTE determination Mashonkina & Zhao (2006) - M06 for common stars.

	ΔT_{eff}	$\Delta \log(g)$	$\Delta [\text{Fe}/\text{H}]$	$\Delta [\text{Ba}/\text{Fe}]$	n
B05	19 ± 76	-0.09 ± 0.19	-0.03 ± 0.08	-0.06 ± 0.07	10
R06	92 ± 29	-0.20 ± 0.24	-0.01 ± 0.04	0.12 ± 0.11	8
M06	12 ± 64	-0.11 ± 0.22	0.01 ± 0.07	0.06 ± 0.08	13

$\log(g)$ declared by Mishenina et al. (2004); and they are rather harmonized for metallicity (within 0.03 dex). The barium abundance ratio difference $\Delta [\text{Ba}/\text{Fe}] = 0.12$, obtained by comparing to the ratio by Reddy et al. (2006) is greater than that received by collating with the other studies; it could be caused by dissimilarity of temperatures and gravities, and maybe by some disparateness of the NLTE and LTE approaches applied in those studies. At the same time, such a shift is within the accuracy limits for the barium abundance determination.

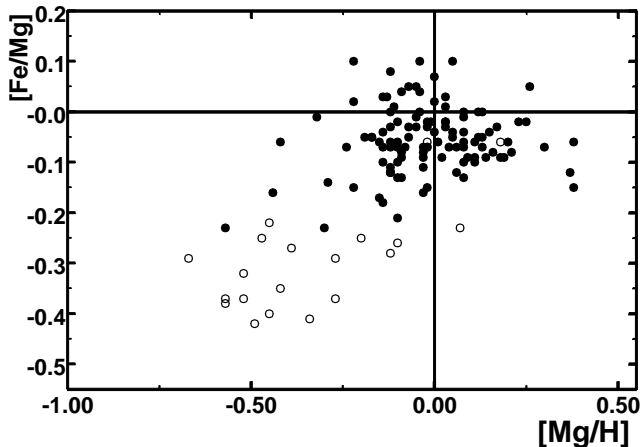


Figure 5. $[\text{Fe}/\text{Mg}]$ vs. $[\text{Fe}/\text{H}]$. The stars of the thin and thick disks are marked as filled and open circles, respectively.

5 DISCUSSION OF THE RESULTS OBTAINED

The obtained barium abundance values are more accurate in view of the NLTE approach application and derivation of stellar models considering distinct chemical compositions of each star; those values are used to analyze the barium abundance in the stars of the thin and thick Galactic discs, assigned by kinematic criteria. The average barium abundances for the thin and thick discs are 0.01 ± 0.08 and -0.03 ± 0.07 , respectively. The average difference is 0.04 dex. To estimate the significance of the difference obtained, we consider the barium abundance variations relative to magnesium - an element that explicitly shows the dissimilarity of abundances in the thick and thin discs (Gratton et al. 2000, Fuhrmann 1998, Mashonkina & Gehren 2001, Bensby et al. 2005, Reddy et al. 2006, Mishenina et al. 2004, etc.) and has the only source of production, namely Supernovae of 8-12 M_{\odot} . To make such a comparison, we can use the magnesium abundances determined under the NLTE approximation in the previous studies (Mishenina et al. 2004) that specified the assignment to the discs.

The relative abundances $[\text{Fe}/\text{Mg}]$ vs. $[\text{Mg}/\text{H}]$ and $[\text{Ba}/\text{Mg}]$ vs. $[\text{Mg}/\text{H}]$ only for the stars of the thick and thin discs are presented in Fig. 5, 6. The dissimilarity between the magnesium abundances in the thick and thin discs is clearly retraced in Fig. 5 that shows the correlation between $[\text{Fe}/\text{Mg}]$ and $[\text{Mg}/\text{H}]$. For the dependence of $[\text{Ba}/\text{Mg}]$ relative to $[\text{Mg}/\text{H}]$ shown in Fig. 6, we observe a barely noticeable trend with the magnesium abundance increasing; the barium underabundance in the thick disc relative to the solar ratio and a "cloud" in the thin disc. That means that the difference in the barium behaviour in the thick and thin discs is retraced more clearly. However, the above may also be evidence of different sources of production of those elements. It should be noted that such comparison is rather relative in this case as the elemental enrichment in the disc stars is contributed by the reproduction by several generations of stars; i.e. there is enough time for the interstellar medium to get enriched with elements produced by numerous predecessors either massive or less massive, including Supernovae and the AGB stars, whose fractions to the enrichment are not proportionate.

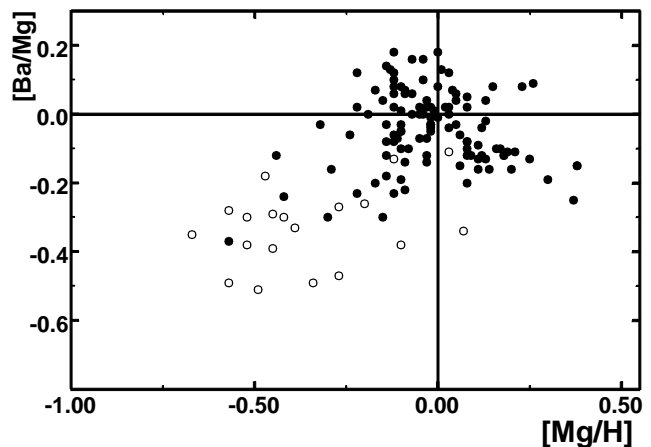


Figure 6. $[\text{Ba}/\text{Mg}]$ vs. $[\text{Mg}/\text{H}]$. The stars of the thin and thick disks are marked as filled and open circles, respectively.

Therefore, to adequately reconstruct the enrichment history, it is necessary to use chemical evolution models that allow for many factors provoking changes in the abundance of one or another chemical element, e.g. elemental production sources, the Galactic structure model, the initial mass function, the star formation rate, etc.

In this work, we are to compare the obtained barium abundances to the computations of the model by Serminato et al. (2009).

It is interesting to make such a comparison by considering several points: 1) what is the s- and r-processes contribution to the barium enrichment at metallicities from -1 to +0.3; 2) what stars (sources) contribute to the barium production the most; 3) whether the barium enrichment in the thick disc differs from that in the thin disc within the bounds of the applied model of the thick disc formation and the Galaxy formation as a whole. In the study by Serminato et al. (2009), firstly, using the FRANEC code (Chiieffi et al. 1998), the s-process contribution to each investigated isotope at the solar system formation epoch was computed following the AGB stars yield only. Then, using the r-process residual method, the r-process fraction was determined for each isotope by subtracting the corresponding s-process fraction; subsequently, the chemical evolution model was recomputed. For example, considering barium, the r-residual of 21% was assumed (Travaglio et al. 1999), the main contributors were Supernovae of type II with masses within $8 < M/M_{\odot} < 12$. The calculations were made on the base of the model by (Ferrini et al. 1992), that allows of the Galaxy division into three components: the halo, the thin and thick discs. In so doing, it was assumed that the thin disc is formed from the matter falling from the halo and the thick disc. The problem of the above model is the fact that the thick disc can not be formed from the halo gas (Wyse & Gilmore 1992). It is not possible to distinguish the thin and thick discs in the two-infall model by Chiappini et al. (1997) either. Therefore, taking into account computations of the Galactic evolution models as of today, we can not clarify the question on the difference of the Galactic discs enrichment with one or another element.

Using the model by Serminato et al. (2009), we can determine the s- and r-processes contributions to the barium

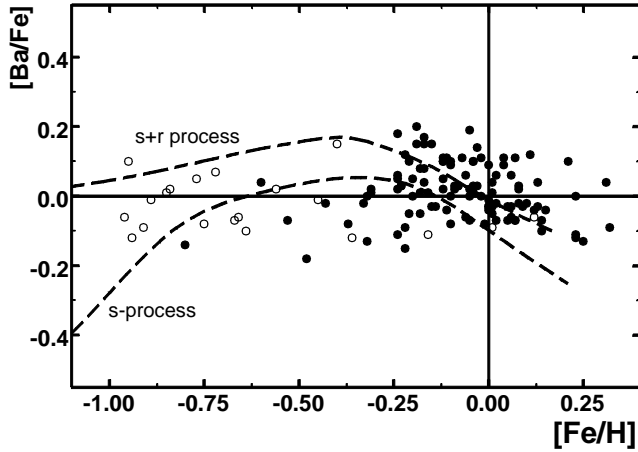


Figure 7. The results of the comparison of the observed trend of $[\text{Ba}/\text{Fe}]$ vs. $[\text{Fe}/\text{H}]$ to the computations of the Galactic chemical evolution (dashed lines) by Serminato et al. (2009).

enrichment with allowance of the s-elements (in particular, barium) production sources applied in the model. It is indicated that the s-elements enrichment at the solar metallicity is contributed mainly by the AGB low-mass stars ($1.5 < M/M_{\odot} < 3$). The results of the comparison of the observed correlation between the barium abundance and metallicity to the calculations of the model by Serminato et al. (2009) are shown in Fig. 7.

It is evident that the observations are poorly specified by the estimated r+s process curve for the thin disc stars with $[\text{Fe}/\text{H}] > 0.1$ dex and $[\text{Fe}/\text{H}] < -0.2$ dex. That means that the r-process contribution differs from that fraction applied in the model by Serminato et al. (2009).

The given comparison indicates that the barium enrichment in the thick and thin discs (at metallicity from -1 to +0.3) is a process more complicated than that specified in the considered model; and it requires further studying.

6 CONCLUSIONS

1. The barium abundance in 172 dwarf stars in the metallicity range from -1 to +0.3 is determined from four lines under the NLTE approximation with distinct atmospheric models.

2. A slight difference (0.04 dex) in the average barium abundances is indicated between the investigated stars, kinematically assigned to the thick (21 stars) and thin (109 stars) discs. However, the dependence of $[\text{Ba}/\text{Mg}]$ vs. $[\text{Mg}/\text{H}]$ has shown different behaviour of the barium abundance in the thick and thin discs.

3. The comparison to the Galactic chemical evolution model by Serminato et al. (2009) has indicated that the barium enrichment is evidently specified by contributions of the s- and r-processes, applied in the model for the stars with metallicity $-0.2 < [\text{Fe}/\text{H}] < 0.1$ dex. However, the r-process contribution in the stars with other metallicity ranges differs from that fraction applied in the Serminato model.

Table 3. Atmospheric parameters and Ba_{NLTE} abundances

HD	T_{eff}	$\log(g)$	$[\text{Fe}/\text{H}]$	$[\text{Ba}/\text{H}]_{\text{NLTE}}$
HD000245	5400	3.4	-0.84	-0.82
HD001562	5828	4.0	-0.32	-0.32
HD001835	5790	4.5	+0.13	+0.17
HD003765	5079	4.3	+0.01	-0.08
HD004307	5889	4.0	-0.18	-0.10
HD004614	5965	4.4	-0.24	-0.22
HD005294	5779	4.1	-0.17	-0.02
HD006582	5240	4.3	-0.94	-1.06
HD008648	5790	4.2	+0.12	+0.08
HD009826	6074	4.0	+0.10	+0.08
HD010145	5673	4.4	-0.01	-0.07
HD010307	5881	4.3	+0.02	+0.00
HD010476	5242	4.3	-0.05	-0.05
HD010780	5407	4.3	+0.04	+0.13
HD011007	5980	4.0	-0.20	-0.15
HD013403	5724	4.0	-0.31	-0.40
HD013507	5714	4.5	-0.02	+0.09
HD013783	5350	4.1	-0.75	-0.83
HD013974	5590	3.8	-0.49	-0.50
HD014374	5449	4.3	-0.09	-0.07
HD017674	5909	4.0	-0.14	-0.17
HD017925	5225	4.3	-0.04	-0.01
HD019019	6063	4.0	-0.17	+0.00
HD019308	5844	4.3	+0.08	+0.07
HD019373	5963	4.2	+0.06	+0.03
HD022049	5084	4.4	-0.15	+0.00
HD022484	6037	4.1	-0.03	+0.00
HD022556	6155	4.2	-0.17	-0.13
HD022879	5972	4.5	-0.77	-0.72
HD023050	5929	4.4	-0.36	-0.40
HD024053	5723	4.4	+0.04	+0.15
HD024206	5633	4.5	-0.08	-0.05
HD028005	5980	4.2	+0.23	+0.23
HD028447	5639	4.0	-0.09	-0.06
HD029150	5733	4.3	+0.00	-0.03
HD029310	5852	4.2	+0.08	+0.10
HD029645	6009	4.0	+0.14	+0.07
HD030495	5820	4.4	-0.05	+0.14
HD030562	5859	4.0	+0.18	+0.20
HD032147	4945	4.4	+0.13	+0.09
HD033632	6072	4.3	-0.24	-0.06
HD034411	5890	4.2	+0.10	+0.09
HD038858	5776	4.3	-0.23	-0.20
HD039587	5955	4.3	-0.03	+0.11
HD040616	5881	4.0	-0.22	-0.10
HD041330	5904	4.1	-0.18	-0.17
HD041593	5312	4.3	-0.04	+0.06
HD043587	5927	4.1	-0.11	-0.15
HD043856	6143	4.1	-0.19	-0.04
HD043947	6001	4.3	-0.24	-0.18
HD045067	6058	4.0	-0.02	-0.02
HD050281	4712	3.9	-0.20	-0.20
HD051419	5746	4.1	-0.37	-0.45
HD055575	5949	4.3	-0.31	-0.29
HD058595	5707	4.3	-0.31	-0.30
HD061606	4956	4.4	-0.12	-0.10
HD062613	5541	4.4	-0.10	-0.10
HD064606	5250	4.2	-0.91	-1.05
HD064815	5864	4.0	-0.33	-0.26
HD065583	5373	4.6	-0.67	-0.74
HD065874	5936	4.0	+0.05	-0.02
HD066573	5821	4.6	-0.53	-0.60
HD068017	5651	4.2	-0.42	-0.54
HD068638	5430	4.4	-0.24	-0.19

Table 3 – continued

HD	T_{eff}	$\log(g)$	[FeH]	[Ba/H] _{NLTE}
HD070923	5986	4.2	+0.06	+0.00
HD071148	5850	4.2	+0.00	-0.01
HD072760	5349	4.1	+0.01	+0.05
HD072905	5884	4.4	-0.07	+0.04
HD073344	6060	4.1	+0.08	+0.06
HD075732	5373	4.3	+0.25	+0.12
HD076151	5776	4.4	+0.05	+0.02
HD076932	5840	4.0	-0.95	-0.85
HD081809	5782	4.0	-0.28	-0.43
HD082106	4827	4.1	-0.11	+0.00
HD088072	5778	4.3	+0.00	-0.03
HD089251	5886	4.0	-0.12	-0.07
HD089269	5674	4.4	-0.23	-0.20
HD091347	5931	4.4	-0.43	-0.45
HD095128	5887	4.3	+0.01	-0.04
HD098630	6060	4.0	+0.22	+0.13
HD101177	5932	4.1	-0.16	-0.15
HD102870	6055	4.0	+0.13	+0.10
HD106516	6165	4.4	-0.72	-0.65
HD107213	6156	4.1	+0.07	+0.09
HD107705	6040	4.2	+0.06	+0.12
HD108954	6037	4.4	-0.12	-0.01
HD109358	5897	4.2	-0.18	-0.23
HD110833	5075	4.3	+0.00	-0.04
HD110897	5925	4.2	-0.45	-0.46
HD112758	5203	4.2	-0.56	-0.78
HD114710	5954	4.3	+0.07	+0.18
HD115383	6012	4.3	+0.11	+0.23
HD116443	4976	3.9	-0.48	-0.66
HD117043	5610	4.5	+0.21	+0.31
HD117176	5611	4.0	-0.03	-0.04
HD117635	5230	4.3	-0.46	-0.50
HD119802	4763	4.0	-0.05	-0.03
HD122064	4937	4.5	+0.07	+0.00
HD125184	5695	4.3	+0.31	+0.35
HD126053	5728	4.2	-0.32	-0.45
HD131977	4683	3.7	-0.24	-0.35
HD135204	5413	4.0	-0.16	-0.27
HD135599	5257	4.3	-0.12	-0.02
HD137107	6037	4.3	+0.00	+0.09
HD139323	5204	4.6	+0.19	+0.19
HD139341	5242	4.6	+0.21	+0.14
HD140538	5675	4.5	+0.02	+0.08
HD141004	5884	4.1	-0.02	-0.02
HD144287	5414	4.5	-0.15	-0.18
HD144579	5294	4.1	-0.70	-0.95
HD145675	5406	4.5	+0.32	+0.23
HD146233	5799	4.4	+0.01	+0.02
HD149661	5294	4.5	-0.04	-0.03
HD151541	5368	4.2	-0.22	-0.37
HD152391	5495	4.3	-0.08	-0.05
HD154345	5503	4.3	-0.21	-0.26
HD154931	5910	4.0	-0.10	-0.09
HD157089	5785	4.0	-0.56	-0.54
HD158633	5290	4.2	-0.49	-0.65
HD159062	5414	4.3	-0.40	-0.25
HD159222	5834	4.3	+0.06	+0.03
HD159482	5620	4.1	-0.89	-0.90
HD159909	5749	4.1	+0.06	-0.05
HD160346	4983	4.3	-0.10	-0.18
HD161098	5617	4.3	-0.27	-0.29
HD164922	5392	4.3	+0.04	-0.05
HD165173	5505	4.3	-0.05	-0.12

Table 3 – continued

HD	T_{eff}	$\log(g)$	[FeH]	[Ba/H] _{NLTE}
HD165341	5314	4.3	-0.08	-0.05
HD165401	5877	4.3	-0.36	-0.48
HD165476	5845	4.1	-0.06	-0.12
HD165670	6178	4.0	-0.10	+0.00
HD165908	5925	4.1	-0.60	-0.56
HD166620	5035	4.0	-0.22	-0.31
HD168009	5826	4.1	-0.01	-0.07
HD173701	5423	4.4	+0.18	+0.08
HD176841	5841	4.3	+0.23	+0.11
HD182488	5435	4.4	+0.07	+0.00
HD182736	5430	3.7	-0.06	-0.01
HD183341	5911	4.3	-0.01	-0.09
HD184499	5750	4.0	-0.64	-0.74
HD184768	5713	4.2	-0.07	-0.16
HD185144	5271	4.2	-0.33	-0.35
HD186104	5753	4.2	+0.05	+0.00
HD186408	5803	4.2	+0.09	+0.06
HD186427	5752	4.2	+0.02	-0.05
HD187897	5887	4.3	+0.08	+0.11
HD189087	5341	4.4	-0.12	-0.02
HD190360	5606	4.4	+0.12	+0.06
HD190404	4963	3.9	-0.82	-1.15
HD191533	6167	3.8	-0.10	-0.01
HD194598	5890	4.0	-1.21	-1.25
HD195005	6075	4.2	-0.06	+0.00
HD195104	6103	4.3	-0.19	+0.01
HD197076	5821	4.3	-0.17	-0.09
HD199960	5878	4.2	+0.23	+0.12
HD201889	5600	4.1	-0.85	-0.84
HD201891	5850	4.4	-0.96	-1.02
HD202108	5712	4.2	-0.21	-0.11
HD203235	6071	4.1	+0.05	+0.00
HD204521	5809	4.6	-0.66	-0.72
HD205702	6020	4.2	+0.01	-0.02
HD208906	5965	4.2	-0.80	-0.94
HD210667	5461	4.5	+0.15	+0.11
HD210752	6014	4.6	-0.53	-0.50
HD211472	5319	4.4	-0.04	+0.06
HD215065	5726	4.0	-0.43	-0.59
HD215704	5418	4.2	+0.07	-0.05
HD217014	5778	4.2	+0.14	+0.04
HD218209	5705	4.5	-0.43	-0.44
HD219134	4900	4.2	+0.05	+0.02
HD219396	5733	4.0	-0.10	-0.19
HD224930	5300	4.1	-0.91	-1.00

ACKNOWLEDGMENTS

This work was supported by the Swiss National Science Foundation, project SCOPES No. IZ73Z0-128180. We thank the referee M. Asplund for valuable comments that improved the paper.

REFERENCES

Allen C.W., 1973, *Astrophysical Quantities* (London: Athlone Press)
 Allende Prieto C., Garca Lpez R.J., Lambert D.L., Gustafsson B., 1999, *ApJ* 527, 879.
 Alonso, A., Arribas, S., & Martínez-Roger, C., 1996, *A&AS* 117, 227

- Andrievsky S.M., Spite M., Korotin S.A. et al., 2009, *A&A*, 494, 1083
- Argast D., Samland M., Thielemann F. K., Qian Y. Z., 2004, *A&A*, 416, 997
- Asplund, M., Grevesse, N., Sauval, A. J., 2005, *ASP Conf. Ser.*, 336, 25
- Barklem P. S., Piskunov N., O'Mara B. J., 2000, *A&AS*, 142, 467
- Baranne A., Queloz D., Mayor M. et al. 1996, *A&AS*, 119, 373
- Blackwell, D.E. & Lynas-Gray, A.E, 1998, *A&A* 129, 505
- Bensby T., Feltzing S., Lundstrom I., Ilyin I., 2005, *A&A*, 433, 185
- Carlsson M., 1986, *Uppsala Obs. Rep.* 33
- Cameron A.G.W., 1982, *Ap&SS* 82, 123
- Castelli, F., Kurucz, R.L., 2004, *arXiv:astro-ph/0405087*
- Cestito G., Francois P., Matteucci et al., 2006, *A&A*, 448, 557
- Chiappini C., Matteucci F., Gratton R., 1997, *Ap.J.*, 477, 765
- Chieffi A., Limongi M., Straniero O., 1998, *ApJ*, 502, 737
- Crandall D.H., Dunn G.H., Gallagher A., Hummer D.G., Kunasz C.V., Leep D., Taylor P.O., 1974, *ApJ* 191, 789
- Cristallo S., Straniero O., Gallino R., Piersanti L., Dominguez I., Lederer M.T., 2009, *Ap.J.*, 696, 797.
- di Benedetto, G.P., 1998, *A&A* 339, 858
- Edvardsson B., Andersen J., Gustafsson B., Lambert D. L., Nissen P. E., Tomkin, J., 1993, *A&A*, 275, 101
- Ferrini F., Matteucci F., Pardi C., Penco U., 1992, *Ap.J.*, 387, 138
- François P., Depagne E., Hill V., Spite M., Spite F., Plez B., Beers T., Andersen J., James G., Barbuy B., Cayrel R., Bonifacio P., Molaro P., Nordström B., Primas F., 2007, *A&A* 476, 935
- Frebel A., 2010, *AN* , 331, 474
- Freiburghaus C., Rosswog S., Thielemann F.K., 1999, *Ap.J.*, 525, L.121
- Fuhrmann K., 1998, *A&A*, 338, 161
- Galazutdinov G. A., 1992, *Preprint SAO RAS.*, 92, 96
- Gratton R. G., Carretta E., Matteucci F., Sneden C., 2000, *A&A*, 358, 671
- Hofsaess D., 1979, *ADNDT* 24, 285
- Kappeler F., Beer H., Wisshak K. et al., 1982, *ApJ*, 257, 821
- Kappeler F., Beer H., Wisshak K., 1989, *Reports on Progress in Physics*, 52, 945
- Katz D., Soubiran C., Cayrel R., Adda M., Cautain R., 1998, *A&A*, 338, 151
- Korotin S.A., Andrievsky S.M., Luck R.E., 1999, *A&A* 351, 168
- Kovtyukh V.V., Soubiran C., Belik S.I., Gorlova N.I., 2003, *A&A* 411, 559
- Kurucz R.L., Furenlid I., Brault J., Testerman L., 1984, *Solar Flux atlas from 296 to 1300 nm*
- Mashonkina L., Bikmaev I., 1996, *ARep* 40, 94
- Mashonkina L.I., Gehren T., Bikmaev I., 1999, *A&A*, 343, 519
- Mashonkina L.I., Gehren T., 2000, *A&A*, 364, 249
- Mashonkina L.I., Gehren T., 2001, *A&A*, 376, 232
- Mashonkina L.I., Zhao G., 2006, *A&A*, 456, 313
- Mashonkina L.I., Gehren T., Shi J., Korn A., Grupp F., 2010, *Proc.IAU, IAU Symposium*, 265, 197
- Mishenina T.V., Kovtyukh V.V., 2001, *A&A*, 370, 951
- Mishenina T.V., Soubiran C., Kovtyukh V. V., Korotin S.A., 2004, *A&A*, 418, 551
- Reddy B.E., Lambert D.L., Allende Prieto C., 2006, *MNRAS*, 367, 1329
- Rutten R.J., 1978, *SoPh* 56, 237
- Schoening T., Butler K., 1998, *A&AS* 128, 581
- Serminato A., Gallino R., Travaglio C., Bisterzo S., Straniero O., 2009, *Publ. Astron. Soc. of Australia.*, 26, 153
- Sobelman I.I., Vainshtein L.A., Yukov E., 1981, *Excitation of Atoms and Broadening of Spectral Lines*, Springer Ser. in Chem. Phys., Berlin, Springer
- Soubiran C., Girard P., 2005, *A&A*, 438, 139
- Steenbock W., Holweger H., 1992, *LNP* 401, 57
- Surman R., McLaughlin G. C., Ruffert M., Janka H.-Th., Hix W. R., 2008, *ApJ* 679, L1
- Travaglio C., Galli D., Gallino R., Busso M., Ferrini F., Straniero O., 1999, *ApJ* 521, 691
- Tsymbal V.V., 1996, *ASP Conf. Ser.*, 108, 198
- van Regemorter H., 1962, *ApJ* 136, 906
- Woosley S. E., Wilson J. R., Mathews G. J., Hoffman R. D., Meyer B.S. 1994, *Ap.J.*, 433, 229
- Wyse R.F.G., Gilmore G., 1992, *AN*, 104, 144

This paper has been typeset from a \TeX / \LaTeX file prepared by the author.